Biosensors and Bioelectronics 24 (2009) 1253–1258

Contents lists available at ScienceDirect

Biosensors and Bioelectronics

journal homepage: www.elsevier.com/locate/bios

Magnetoresistive immunosensor for the detection of *Escherichia coli* O157:H7 including a microfluidic network

M. Mujika[a,*], S. Arana[a], E. Castaño[a], M. Tijero[b], R. Vilares[b], J.M. Ruano-López[b], A. Cruz[c], L. Sainz[c], J. Berganza[c]

[a] *CEIT-IK4, Paseo de Manuel Lardizábal, No. 15, 20.018 Donostia-San Sebastián, Spain*
[b] *IKERLAN-IK4, Paseo J. M. Arizmendiarrieta 2, 20.500 Mondragón, Spain*
[c] *GAIKER-IK4, Technological Centre, Parque Tecnológico, Ed. 202, 48.170 Zamudio, Spain*

ARTICLE INFO

Article history:
Received 14 April 2008
Received in revised form 15 July 2008
Accepted 15 July 2008
Available online 25 July 2008

Keywords:
Biosensor
Antibodies
Magnetic microspheres
E. coli O157:H7
GMR multilayer

ABSTRACT

A hand held device has been designed for the immunomagnetic detection and quantification of the pathogen *Escherichia coli O157:H7* in food and clinical samples. In this work, a technology to manufacture a Lab on a Chip that integrates a 3D microfluidic network with a microfabricated biosensor has been developed. With this aim, the sensing film optimization, the design of the microfluidic circuitry, the development of the biological protocols involved in the measurements and, finally, the packaging needed to carry out the assays in a safe and straightforward way have been completed. The biosensor is designed to be capable to detect and quantify small magnetic field variations caused by the presence of superparamagnetic beads bound to the antigens previously immobilized on the sensor surface via an antibody–antigen reaction.

The giant magnetoresistive multilayer structure implemented as sensing film consists of 20[$Cu_{5.10\,nm}/Co_{2.47\,nm}$] with a magnetoresistance of 3.20% at 235 Oe and a sensitivity up to 0.06 Ω/Oe between 150 Oe and 230 Oe. Silicon nitride has been selected as optimum sensor surface coating due to its suitability for antibody immobilization.

In order to guide the biological samples towards the sensing area, a microfluidic network made of SU-8 photoresist has been included. Finally, a novel packaging design has been fabricated employing 3D stereolithographic techniques. The microchannels are connected to the outside using standard tubing. Hence, this packaging allows an easy replacement of the used devices.

1. Introduction

In recent years, the evolution of pathogen detection and diagnosis techniques has originated a new series of requirements that leads directly to the search of the simplification of several standard medical processes and treatments. In this sense, the idea of integrating current diagnosis techniques into a simple and portable device has been reinforced, promoting the development of the lab on a chip (LOC) concept. Efforts have been focused on the detection and quantification of specific infectious biological specimens in food samples, a task that requires reliability and short processing periods in order to obtain high efficiency.

According to these needs, immunomagnetic sensors are expected to arise as a remarkable solution for this kind of diagnosis. Therefore, a magnetic sensor has been proposed to act as the core of a biosensor based on the immobilization of antigens (via an antibody–antigen reaction) onto the sensing surface. It has been designed to be capable to detect and quantify small magnetic field variations caused by the presence of superparamagnetic beads bound to the immobilized antigens. For this purpose, *Escherichia coli* O157:H7 (Morandi et al., 2003) has been selected as the target infectious agent to be detected in this work. This pathogen is present in several food categories, particularly in undercooked meat and raw milk and it often causes hemorrhagic colitis.

Fig. 1 shows a schematic diagram of the immunomagnetic detection principle. Immobilization is an essential step of the detection process since the biofunctionalization of the sensing surface provides the way to capture the biological target onto the biosensor. Thus, the specific antibodies, properly located on the sensor surface, capture the target bacteria when the sample subjected to analysis flows through the microchannels. Once the binding of the bacteria to the surface of the sensor has occurred, specific antibody-coated superparamagnetic beads circulate through the detection system (Gehring et al., 2005) binding the antigens again, so that

* Corresponding author. Tel.: +34 943 212 800; fax: +34 943 213 076.
E-mail address: mmujika@ceit.es (M. Mujika).

0956-5663/$ – see front matter © 2008 Elsevier B.V. All rights reserved.
doi:10.1016/j.bios.2008.07.024

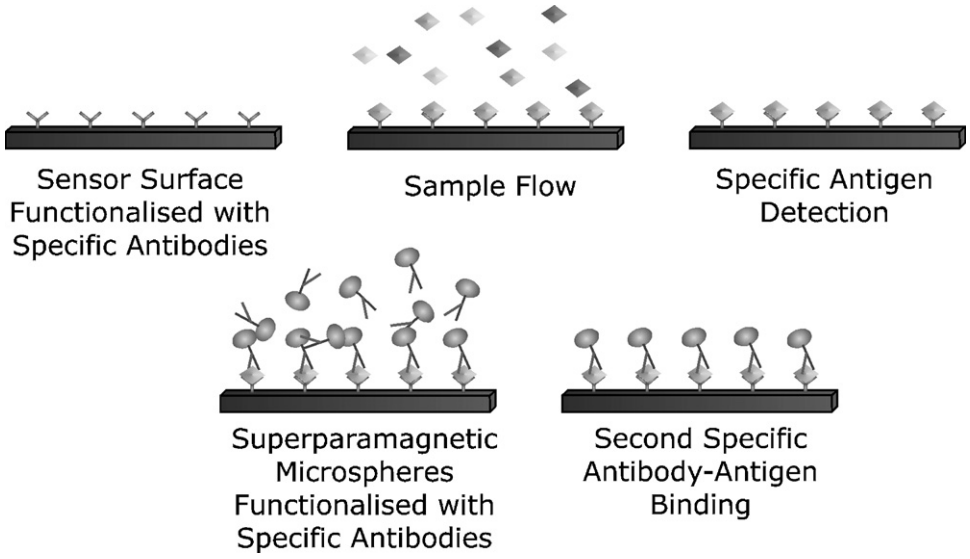

Fig. 1. Schematic flow chart of the detection principle.

an antibody–antigen–antibody sandwich structure, with attached microspheres, is obtained. Finally, an external magnetic field is applied to measure the response of the magnetic sensor. Due to the magnetic dipoles induced by the beads under such field, it is possible to detect the presence of these microparticles located on the active surface of the sensor and, in consequence, the detection of the analysed biological specimen.

In order to be able to detect the stray field of the immobilized microbeads, a multilayered giant magnetoresistance (GMR) has been selected as sensing element. Although there are many types of magnetic sensors, namely Hall sensors or GMI devices, more extensive work has been developed on magnetoresistive transducers with successful results in biological assays (Rife et al., 2003; Graham et al., 2003). The high sensitivity of GMRs at low magnetic fields makes them suitable for the intended goal of the presented work.

With the aim of supplying the samples along the sensing surface, a microfluidic network has been designed and fabricated. Due to the fact that microfluidic devices require the development of thick structures with high aspect ratio, the application of EPON SU-8 epoxy negative photoresist by UV photolithography method has become very popular in MEMS community (Tay et al., 2001; Ruhmann et al., 2002; Agirregabiria et al., 2004; Blanco et al., 2004). This technology is compatible with CMOS processes and multilayer structures can be patterned in a single photolithographic step with standard mask aligners. Furthermore, SU-8 presents interesting properties, such as thermal and chemical stability, good transparency, excellent mechanical, fluidic, optical and electrical properties, and biocompatibility (Voskerician et al., 2003), that make it specially attractive for several applications. Moreover, some of its attributes/characteristics, namely hydrophilicity, fluorescence, refractive index, and magnetism, could be modified by different techniques (Wu et al., 2003; Helbo et al., 2004; Damean et al., 2005). These excellent features make it a popular choice as structural material for the fabrication of MEMS devices.

Considering that the interaction of an antibody with an antigen forms the basis of all immunochemical techniques, the sensor surface should be functionalized with specific antibodies against the target pathogen in order to make it biologically active. Antibodies are a large family of glycoproteins, which are produced by B cells in response to the presence of foreign molecules and are characterised by their ability to bind antigens. The region of the antibody that reacts with the antigen is called the paratope. The region of an antigen that interacts with an antibody is defined as an epitope. Affinity is the measure of the strength of the binding of an epitope to an antibody. Avidity is a measure of the overall stability of the complex between antibodies and antigens.

There are two types of antibodies, polyclonal and monoclonal antibodies, attending their specificity of epitope binding. Monoclonal antibodies are identical monospecific antibodies (which means they show singular epitope specificity) derived from a single B cell line, whereas polyclonal antibodies are a mixture of immunoglobulin molecules secreted against a specific antigen (each recognising a different epitope) derived from different B cell lines. The way they are obtained sets a clear difference between monoclonal and polyclonal antibodies as well. The latter type is produced by injecting an antigen into a mammal (such as a mouse, rat or rabbit for small quantities of antibody, or goat, sheep, or horse for large quantities of antibody). Repeated immunizations of the same antigen at intervals of several weeks stimulate specific B cells to generate large amounts of specific antibodies against the antigen, so that multiple antibodies that bind the same antigen can be derived when isolating the blood of the animals. On the other hand, in order to obtain monoclonal antibodies, antibody-secreting lymphocytes are isolated from the animal and immortalized by fusing them with a cancer cell line. The fused cells, called hybridomas, will continually grow and secrete antibody in culture. Single hybridoma cells are isolated to generate cell clones that all produce homogeneous antibodies with defined specificity.

Monoclonal antibodies are recommended for the detection of highly expressed proteins and for applications, such as flow cytometry, where, in order to prevent false positives, exact target binding is an important requirement. In contrast, polyclonal antibodies are more suitable for the detection of proteins with lower expression levels: considering that more antibodies can bind a single protein molecule, an enhanced detection signal can be achieved (Santa Cruz Biotechnology Inc., 2007).

Antibodies have become a necessary tool to identify and enrich specific molecules in a number of contexts, i.e., enzyme-linked immunosorbant assay (ELISA), Western blot (WB), immunoprecipitation (IP), flow cytometry and FACS, immunohistochemistry (IHC), chromatin immunoprecipitation (ChIP) Assays and immunostaining of cells and tissues. Their ability to bind specific targets, such as proteins and microorganisms and the accuracy and sensitivity

of antibody based detection techniques (Harlow and Lane, 1996; Goding, 1996; Benjamini and Leskowitz, 1991; Hudson and Hay, 1989), lead to their use in detection techniques in the field of medicine, biochemistry, food safety, and environmental research.

As it has already been said when describing the detection principle, magnetic microspheres play an essential role in the immunomagnetic assays. Superparamagnetic particles have been broadly used for the capture of biomolecules and cells in diagnosis and other research applications (namely cell separation, nucleic acid purification or bacterial capture) owing to the benefits they provide, i.e. simplicity for separation assays and suitability for automation. They currently allow the performance of magnetic immunoassays, where the specific affinity against the target is accomplished by the antibodies attached to their own surface. The resulting target-bead structure can be handled by the application of external magnetic fields due to the core of iron oxide (Fe_2O_3, Fe_3O_4) of part of the microspheres. The magnetic behaviour of these particles allows the unbound sample constituents to be efficiently washed away.

Compared to other detection methods, like the ones based on fluorescent markers or electrochemical measurements, the use of magnetic particles provides some remarkable advantages. The constituent compounds of the most usual target samples show an essentially non-magnetic behaviour, which minimizes the noise and possible interferences in the measurement (Larsson et al., 1999). Moreover, the magnetic properties of the beads have long term stability, so that the assays could be repeated as many times as needed. Additionally, controlled movement and positioning of the microspheres is made feasible by applying an external magnetic field gradient.

2. Materials and methods

2.1. Magnetoresistive sensor

A series of multilayered copper–cobalt structures has been fabricated by means of DC magnetron sputtering (Pfeiffer Classic) from high purity copper and cobalt targets onto thermally oxidized silicon wafers (4 in. diameter, 450 μm thick). With the aim of optimizing the multilayered configuration, several samples have been grown at room temperature with different layer thicknesses, ranging from 1.60 nm to 6.60 nm for the copper, whereas the cobalt thickness varies between 1.84 nm and 4.36 nm. In order to obtain meander-like magnetoresistances, the thin film has been patterned via lift-off photolithography techniques. The same techniques have allowed the definition of platinum contacts deposited by DC magnetron sputtering (Edwards ESM-100). In a second processing step, the samples have been annealed for 2 h at 300 °C in a mixture of N_2 and H_2 that prevents oxidation. Finally, a Si_3N_4 layer has been deposited by means of PECVD (Plasmalab 80+, Oxford).

2.2. Sensor layout

The sensor is a 16 mm × 21 mm chip which consists of 16 magnetoresistive meanders placed in groups of four along four parallel SU-8 microchannels. This configuration permits fulfilling the redundancy requirements associated with this type of measurement. Three different sensor geometries have been included in this layout with a line width of 25 μm and total lengths between 3.3 mm and 8 mm. The first design (in the following referred as circular) consists of a circular shape meander along the channel direction, which does not differ much from the second design (rectangular) where the meander has been patterned with a rectangular shape. The third design (longitudinal) is also based on a rectangular shape, but this time it is placed parallel to the channel. The distribution of the different meanders along the channel is the same for every channel: and it begins with a circular meander, then a rectangular one, then a longitudinal geometry, and finally a second circular meander. Contact paths are 0.2 mm wide and each of the 22 pads covers an area of 1.1 mm × 1.1 mm.

2.3. Microfluidic circuitry: design and fabrication

Two different microfluidic network designs have been proposed: one, with one inlet and one outlet, and the other one, with two inlets and two outlets. An aspect to bear in mind deals with delivering the same flow to all sensors. The same flow rate of sample must go through all microfluidic channels in order to get a reliable sensor measurement. The first design, assures the same velocity of flow in all microchannels, but it does not allow to discriminate between the signal and the noise. On the other hand, the second Y shaped design (Fig. 2a) allows the use of a reference channel and assures the same sample flow through all channels.

For the fabrication of the microchannels, two commercially available SU-8 photoresists, SU-8 50 and SU-8 5, have been used with propylene-glycol-monoether-acetate (PGMA) as developer (Microchem Corp.). The auxiliary polyimide film consists of a 125 μm thick Kapton film (Goodfellow, UK) whereas four inch Pyrex wafers (750 μm thick) have been selected as substrates. Positive photoresist S1818 from Shipley acts as adhesive layer between Kapton and Pyrex. Isopropanol (IPA) from Aldrich has been employed to rinse the samples. The photomasks have been generated using a layout software and printed on a plastic film photomask by a photoplotter of 64 000 dpi (J.D. Photo-Tools Ltd., UK).

The fabrication process employed here to manufacture complex 3D multilayer microstructures is based on a full wafer polymer bonding process using two patterned SU-8 layers on separate wafers (Agirregabiria et al., 2005). The process, consists of the following steps: (i) substrate preparation, (ii) photolithography of two SU-8 50 layers, (iii) bonding the two layers and finally, (iv) release of the temporary film.

For a strong adhesion between SU-8 50 and the bottom substrate (silicon nitride, silicon, or silicon oxide), it has been necessary to dehydrate the substrate at 200 °C for a period of 2 h. If the substrate is sufficiently dehydrated, the adhesion will be good, but if it too much time elapses between dehydration and SU-8 spin coating, the adhesion will be very poor due to superficially adsorbed water. Afterwards, a SU-8 50 layer has been deposited on the substrate by spin coating. The height of the SU-8 layers deposited on the substrate also affects the adhesion process in such a way that a highly polymerised SU-8 5 layer allows the enhancement of the adherence between the SU-8 50 and the substrate. Subsequently, a SU-8 50 layer has been processed on the bottom substrate in order to define the fluidic channel width and height. To enclose the microfluidic network, a 125 μm thick Kapton film has been bonded on a transparent substrate. The low adhesion between the Kapton film and the SU-8 allows the film to be released after the bonding process. A new layer of SU-8 50 has been deposited by spin coating on the Kapton and finally patterned. In the next step, the two SU-8 layers have been aligned and introduced into a substrate-bonding machine. Finally, the SU-8 stack has been detached from the Kapton film so that the final device has been obtained.

This novel fabrication process carried out at wafer level allows the obtaining of a 3D microfluidic network, with perfectly sealed channels and reservoirs with heights from 20 μm up to 180 μm. Since all the layers of the chip are photopatternable, the input and output of the microchannels are easily in contact with the outside after the releasing step of the Kapton. The fabrication procedure described above is fast, reproducible, CMOS compatible, and easily

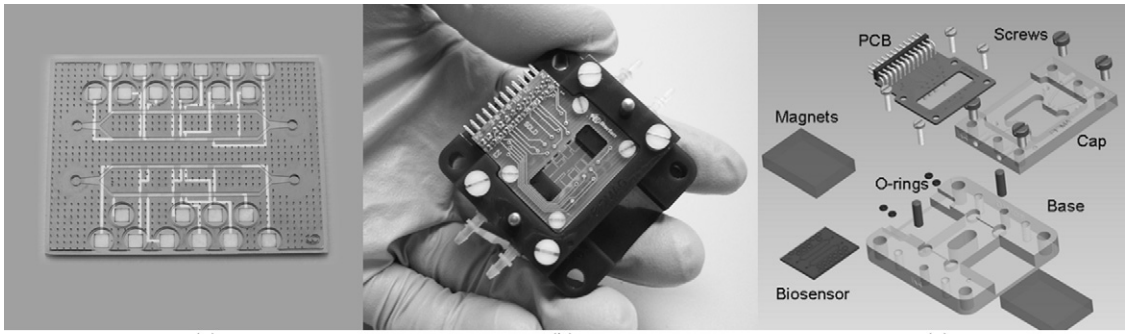

Fig. 2. (a) Sensor element including microfluidic networks with two inlets/outlets. (b) Packaged biosensor ready to be tested. (c) 3D schematic of biosensor packaging design (PROE).

implementable using standard photolithography and bonding equipment. Moreover, this process facilitates the integration of 3D microfluidic networks with any microfabricated biosensor to manufacture a Lab On a Chip.

2.4. Biological protocols

In order to select the proper antibodies, several Sandwich ELISA assays have been carried out. The pursued aim is to measure the amount of antigen between two antibody layers (i.e. capture and detection antibody) and, to achieve this goal, the following materials have been used:

2.4.1. Antibodies

Antibody specific against *E. coli* O157:H7, from Chemicon.
Secondary antibody rabbit polyclonal to mouse IgG + IgM + IgA (HRP), from Abcam.

2.4.2. Bacterial cultures to evaluate the specificity of the antibodies

E. coli O157:H7 (EDL 933).
E. coli (ATCC 10536).
Salmonella choleraesuis (CECT 443).

2.4.3. Magnetic microspheres

Dynabeads coated with anti-*E. coli* O157:H7, from Dynal.
3,3′,5,5′-Tetramethylbenzidine, from Sigma.

Samples (5 mm × 5 mm) of the different materials: SU-8, silicon dioxide (SiO_2) and silicon nitride (Si_3N_4), have been submerged into serially diluted 10-fold antibody solutions from a starting concentration of 10 μg/ml. Antibody binding to the material surface has been evaluated using an enzyme horseradish peroxidase (HRP) conjugated secondary antibody (rabbit polyclonal to mouse IgG + IgM + IgA + HRP) and developed with tetramethyl benzidine (TMB). Absorbance at 450 nm is directly proportional to the amount of antibody attached to the chip surface.

2.5. Final setup

Pursuing the idea of a hand held device, the whole system has been mounted in an external packing based on two plastic capsules pressed together by means of screws (Fig. 2b). This novel packaging has been designed by a computer aided design tool (Pro Engineer CAD software, PROE) and fabricated using a stereolithography equipment. The combination of these two tools provides a versatile and easy way to fabricate different package prototypes, which can be quickly adapted to successive microfluidic circuits or biosensor designs.

The bottom capsule acts as support for the biosensor, whereas the top capsule contains an O-ring per reservoir to avoid liquid leakage and acts as well as support for the printed circuit board (PCB). This PCB contains metal pins, which are the connection between the electrodes of the biosensor and the pads of the PCB. All the pieces of the packaging are aligned and held together by screws without an adhesive, allowing an easy replacement of the device. The package permits the user to insert the sample through external flexible tubes by a simple syringe (Fig. 2c).

3. Results and discussion

3.1. Magnetoresistive sensor

In multilayered structures constituted by alternative non-magnetic and magnetic layers, the oscillation of the antiferromagnetic interlayer exchange coupling between ferromagnetic and antiferromagnetic configurations depends on the thickness of the spacer layer (Grünberg et al., 1986). In the presented film this spacer layer is made of copper whereas cobalt constitutes the magnetic layer. Bearing this in mind and intending to determine the optimal copper layer thickness (Hütten et al., 1999), several samples have been fabricated with thicknesses within 1.60 nm and 6.60 nm, for a given cobalt thickness. The magnetoresistance of this series at 253 Oe varies from 0.18% to 0.93%. Following a similar procedure, different cobalt thicknesses, comprised between 1.84 nm and 4.36 nm, have been considered for a given copper thickness. In this case, the magnetoresistance at 235 Oe oscillates between 0.91% and 1.35%.

Regarding the magnetoresistive performance, a copper thickness of 5.10 nm (Giron et al., 1993) has been determined to be the one showing the best performance. For this spacer layer thickness, the optimal response corresponds to a 2.47 nm cobalt layer (Heitmann, 2004). Summarising, the selected multilayer structure consists of $20[Cu_{5.10\,nm}/Co_{2.47\,nm}]$ with a magnetoresistance amplitude of 1.35% at 235 Oe.

After annealing, as well as a better response with an amplitude of 3.20% at 235 Oe, a higher thermal stability has also been achieved. Furthermore, due to a non-optimized magnetic microstructure, the samples in the "as-deposited" state are not able to recover the initial resistive value. While being subjected to the external field, the multilayered structure is magnetized, which is the phenomenon

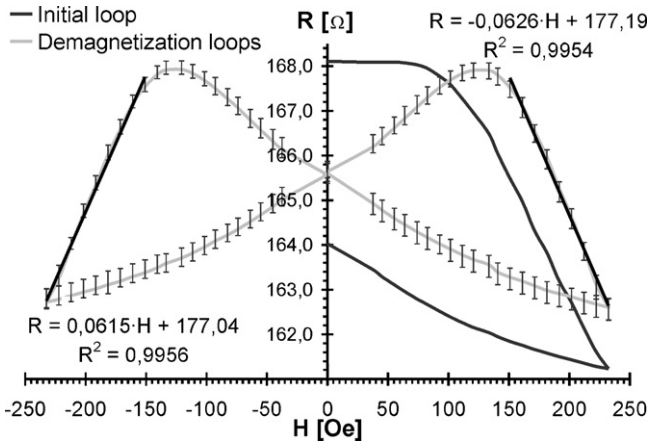

Fig. 3. Linear measurement ranges with a sensitivity up to 0.06 Ω/Oe between 150 Oe and 230 Oe and a magnetoresistance scope of about 3.2% at 230 Oe.

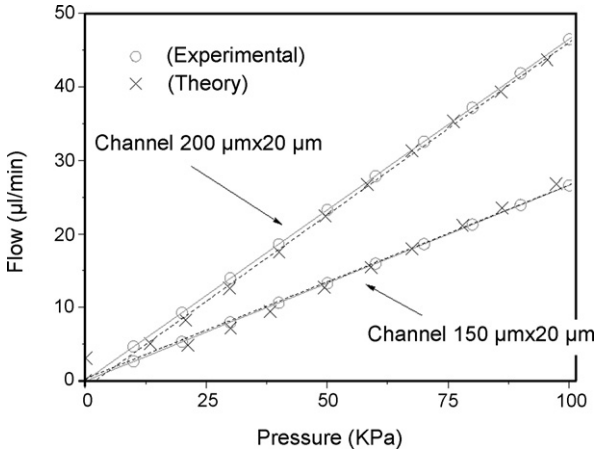

Fig. 5. Experimental flows at different injection pressures (solid lines) versus theoretical flows (dash lines).

responsible for the non-reversible response. On the other hand, the resistance of the annealed samples after demagnetization is in good agreement with its initial value, as depicted in Fig. 3.

Results reported by other groups suggest that, when subjected to an external magnetic field up to 500 Oe, the magnetic beads are capable of inducing a resistance variation of about 0.1% (Brzeska et al., 2004; Brückl et al., 2005). Considering that the maximum in-plane stray field associated to such beads is typically ranged around 10–40 Oe (Schotter et al., 2004), it is expected a minimum resistance variation of about 0.36% for the proposed sensor at around 200 Oe.

Related to the influence of the meander geometry, clear differences have been detected in the magnetoresistive performance of the samples as can be seen in Fig. 4. The lowest response, regarding the maximum magnetoresistance and the sensitivity at low fields, corresponds to the longitudinal design, whereas the highest values for these parametres have been shown by the rectangular design. Both, the magnetoresistance at 235 Oe and the sensitivity up to the same external field magnitude, are about 3.5 times higher for the rectangular design as for the longitudinal one.

3.2. Microfluidic circuitry

The microchannels fabricated following the developed processes have been tested with DI water and have shown an excellent sealing as can be seen in Fig. 5. These graphs represent the flow of DI water at various pressures from 0 KPa to 100 KPa within channels of 20 µm height and 200 µm and 150 µm of width. Theoretical results predicted (dash lines) by fluid macroscopic theory have been compared to experimental measurements (solid lines) and it has been concluded that the fluid behaviour is in agreement with the theoretic results.

In order to facilitate the optical detection of equal flow, the microfluidic tests have been carried out at a low pressure of 50 KPa and a blue dyed liquid has been chosen as the sample. It has been successfully proved that the liquid advances at the same flow rate in all channels without leaks.

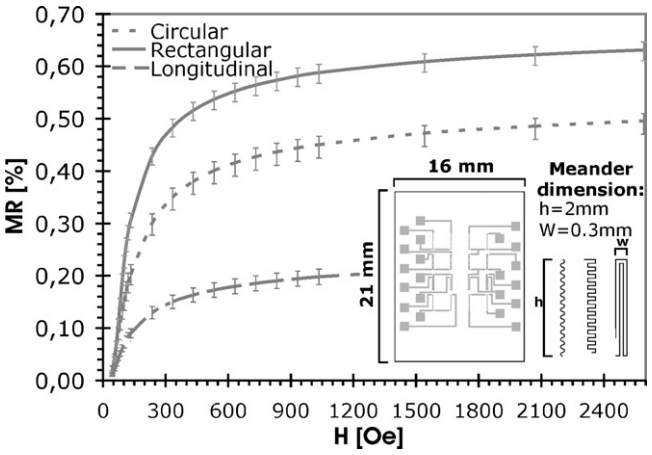

Fig. 4. Layout design including different geometries considered and their influence in the magnetoresistance.

3.3. Biological protocols

With the purpose of selecting the proper antibodies for *E. coli* O157:H7 detection, several sandwich ELISA assays have been carried out. This kind of assay is based on the principles of antibody/antigen interaction as described in the following. The labelling of an antibody with an enzyme by chemical conjugation allows the detection of immune complexes on a solid phase (ELISA plate). Once the enzyme is fixed and free of excess reagents, it reacts with a substrate to yield a coloured product which can be visualized. The pursued aim is to measure the amount of antigen between two antibody layers (i.e. capture and detection antibody). The specificity of the selected antibody has been tested with the target bacteria, *E. coli* O157:H7, and other analogous microorganisms (non-pathogenic *E. coli* and *Salmonella* spp.). The obtained results have shown high specificity for *E. coli* O157:H7 (10^5 colony forming units/ml), whereas non-pathogenic *E. coli* has been detected only in high concentrations (10^7 colony forming units/ml), as shown in Fig. 6a. In addition, the negative control, *Salmonella* spp., has not been detected at any concentration.

In order to choose a suitable material for immobilization on the sensor surface, the absorption of the specific antibody to *E. coli* O157:H7 has been evaluated via ELISA assays. Three possible materials have been taken into account and compared to polystyrene (used as the control material): SU-8, silicon dioxide (SiO_2) and silicon nitride (Si_3N_4). The highest absorption of the antibody on sensor surface corresponds to the silicon nitride, as depicted in Fig. 6b. The selection of the most appropriate surface material for antibody immobilization has been the main aim of these measurements, therefore no further search has been carried out in order to determine the binding mechanisms between the different materials and the antibodies.

(a)

Colony forming units/ml	Absorbance at 450 nm		
	E. coli O157:H7	Non pathogenic *E. coli*	*Salmonella* spp
10^9	1,22	0,36	0,13
10^7	0,56	0,21	0,09
10^5	0,27	0,09	0,14
10^3	0,10	0,12	0,08

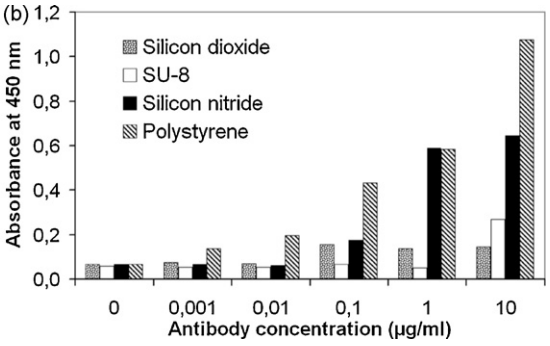

Fig. 6. (a) Specifity of the antibody and (b) antibody absorption on materials.

4. Conclusions

A new, portable microsystem has been designed for the immunomagnetic detection of the pathogen *E. coli* O157:H7 in food and clinical samples. With this purpose, a low magnetic field sensor based on giant magnetoresistive multilayer structures has been developed into a four-channel configuration that provides redundancy in measurements. The structure consists of $20[Cu_{5.10\,nm}/Co_{2.47\,nm}]$ with a magnetoresistance of 3.20% at 235 Oe and a sensitivity up to 0.06 Ω/Oe between 150 Oe and 230 Oe. It is expected a minimum resistance variation of about 0.36% for the proposed sensor at around 200 Oe. Silicon nitride has been selected as optimal sensor surface coating due to its suitability for antibody immobilization.

In order to guide the biological samples towards the sensing area, a microfluidic network made of a SU-8 photo resist network has been integrated. Finally, a novel packaging design has been fabricated employing stereolithographic techniques. The microchannels are connected to the outside using standard tubing. Hence, this packaging device allows an easy replacement of the used devices.

Acknowledgements

The authors acknowledge the Spanish Ministry of Education and Science for funding this research and Bask Government's grant promoting doctoral theses for young pre-doctoral researchers.

References

Agirregabiria, M., Blanco, F.J., Berganzo, J., Ruano-López, J.M., Aramburu, I., García, J., Mayora, K., 2004. Proceedings of Eighth Internacional Conference on Miniaturized Chemical and Biochemical Analysis Systems, vol. 2, Malmö, Sweden, pp. 49–51.

Agirregabiria, M., Blanco, F.J., Berganzo, J., Arroyo, M.T., Fullaondo, A., Mayora, K., Ruano-López, J.M., 2005. Lab on a Chip 5, 545–552.

Benjamini, E., Leskowitz, S. (Eds.), 1991. Immunology: A Short Course, 2nd ed. Wiley–Liss, New York.

Blanco, F.J., Agirregabiria, M., García, J., Berganzo, J., Tijero, M., Arroyo, M.T., Ruano-López, J.M., Aramburu, I., Mayora, K., 2004. J. Micromech. Microeng. 14, 1047–1056.

Brückl, H., Panhorst, M., Schotter, J., Kamp, P.B., Becker, A., 2005. IEE Proc. Nanobiotechnol. 152, 41–46.

Brzeska, M., Panhorst, M., Kamp, P.B., Schotter, J., Reiss, G., Pühler, A., Becker, A., Brückl, H., 2004. J. Biotechnol. 112, 25–33.

Damean, N., Parviz, B.A., Lee, J.N., Odom, T., Whitesides, G.M., 2005. J. Micromech. Microeng. 15, 29–34.

Gehring, A.G., et al., 2005. J. Food Prot. 68, 146–149.

Giron, F., Boher, P., Houdy, Ph., et al., 1993. J. Magn. Magn. Mater. 121, 318–321.

Goding, J.W. (Ed.), 1996. Monoclonal Antibodies: Principles and Practice, 3rd ed. Academic Press, New York.

Graham, D.L., Ferreira, H.A., Freitas, P.P., Cabral, J.M.S., 2003. Biosens. Bioelectron. 18, 483–488.

Grünberg, P., Schreiber, R., Pang, Y., Brodsky, M.B., Sowers, H., 1986. Phys. Rev. Lett. 57, 2442–2445.

Harlow, E., Lane, D. (Eds.), 1996. Antibodies—A Laboratory Manual. Cold Spring Harbor Laboratory.

Heitmann, S., 2004. Cobalt/copper multilayers: interplay of microstructure and GMR and recrystallization as the key towards temperature stability. PhD. Thesis.

Helbo, B., Kragh, S., Kjeldsen, B.G., Reimers, J.L., Kristensen, A., 2004. Sens. Actuators A 111–1, 21–25.

Hudson, L., Hay, F.C. (Eds.), 1989. Practical Immunology, 3rd ed. Blackwell Scientific Publications, Oxford.

Hütten, A., Mrozek, S., Heitmann, S., Tempel, T., Brückl, H., Reiss, G., 1999. Acta Mater. 47, 4245–4252.

Larsson, K., Kriz, K., Kriz, D., 1999. Analysis 27, 617–621.

Morandi, E., Grassi, C., Cellerino, P., Massara, P., Corsi, F., Trabucchi, E., 2003. J. Clin. Gastroenterol. 36, 44–46.

Rife, J.C., Miller, M.M., Sheehan, P.E., Tamanaha, C.R., Tondra, M., Whitman, L.J., 2003. Sens. Actuators A 107, 209–218.

Ruhmann, R., Pfeiffer, K., Falenski, M., Reuther, F., Engelke, R., Grützner, G., 2002. Mstnews 1, 45–46.

Schotter, J., Kamp, P.B., Becker, A., Pühler, A., Reiss, G., Brückl, H., 2004. Biosens. Bioelectron. 19, 1149–1156.

Tay, F.E.H., Van Kan, J.A., Watt, F., Choong, W., 2001. J. Micromech. Microeng. 11, 27–32.

Voskerician, G., Shive, M.S., Shawgo, R.S., von Recum, H., Anderson, J.M., Cima, M.J., Langer, R., 2003. Biomaterials 24, 1959–1967.

www.scbt.com/antibody.html, Santa Cruz Biotechnology, 2007–2008.

Wu, C.L., Chen, M.H., Tseng, F.G., October 2003. Proceedings of Seventh International Conference on Miniaturized Chemical and Biochemical Analysis Systems, Squaw, Valley, USA, pp. 1117–1120.